van der Waals corrections to density functional theory calculations: Methane, ethane, ethylene, benzene, formaldehyde, ammonia, water, PBE, and CPMD

2 AUTHORS, INCLUDING:

Robert Wayne Williams
Uniformed Services University of the Healt…

83 PUBLICATIONS **2,690** CITATIONS

ELSEVIER

van der Waals corrections to density functional theory calculations: Methane, ethane, ethylene, benzene, formaldehyde, ammonia, water, PBE, and CPMD ☆

Robert W. Williams *, Daksh Malhotra

Department of Biomedical Informatics, Uniformed Services University, 4301 Jones Bridge Road, Bethesda, MD 20815, United States

Abstract

Parameters are developed for a practical application of the empirical van der Waals (vdW) correction infrastructure available in the CPMD density functional theory (DFT) code. The binding energy, geometry, and potential energy surface (PES) are examined for methane, ethane, ethylene, formaldehyde, ammonia, three benzene dimer geometries, and three benzene–water geometries. The vdW corrected results compare favorably with MP2 and CCSD(T) calculations near the complete basis set limits, and with experimental results where they are available.
Published by Elsevier B.V.

Keywords: Ab initio; van der Waals; Dispersion; Empirical corrections; BLYP; PBE; CPMD; Quantum mechanical; DFT; Density functional theory; Methane; Ethane; Ethylene; Formaldehyde; Ammonia; Benzene; Water

1. Introduction

Density functional theory (DFT) has provided a poor description of van der Waals (vdW) forces. This has limited its usefulness in a variety of problems that include the study of organic molecular crystals, amino acid, polypeptide and DNA structure, protein–ligand interactions, and structure based drug design. Most of the widely available density functionals yield repulsive forces only, or binding energies and geometries that are significantly in error [1]. Even those functionals that provide qualitatively accurate attractive forces below 5 or 6 Å show a binding energy that rises above zero to become repulsive at longer separations [2].

Efforts to develop DFT methods that provide more quantitative descriptions of non-bonded interactions have been under way for several years [3]. Relatively accurate results have recently been reported for the new X3LYP

functional [4]. Other efforts to improve this situation have been aimed at providing empirical corrections to DFT calculations, and those results have been reported to be "comparable" [5,6] or "even superior to" [7] MP2 calculations in many cases. Most recently it has been shown that very accurate vdW corrections can be obtained from C_6 coefficients and low temperature crystal structures [8]. These approaches also offer a solution to the problem associated with repulsive forces above five to six angstroms using most density functionals. However, Zimmerli et al. [9] have cautioned that appropriate combinations of the damping functions and density functionals available in various codes have "to be tailored to the problem in question". A C_6 scale factor introduced by Grimme [7] makes the task of tailoring quite flexible.

The heart of the empirical correction scheme is a damping function, multiplied by a diatomic vdW strength coefficient, $C_6^{\alpha\beta}$, and divided by R^6. Numerous different damping functions have been employed. The only function presently implemented in CPMD is given by Elstner et al. [5],

$$f(\mathbf{R}) = \left(1 - \exp\left[-d\left(\frac{R_{ij}^{\alpha\beta}}{R_0^{\alpha\beta}}\right)^7\right]\right)^4. \tag{1}$$

This equation has the same form as that constructed by Mooij et al. [10], and later used by Wu and Yang [6], where the inner and outer exponents are 3 and 2, respectively. The exponents used by Elstner et al. and here, 7 and 4, ensure that the effect of the vdW correction drops to zero around 3 Å, so that bonded interactions are not included.

The vdW energy, added to the total energy of the system, is then

$$E_{vdW} = \sum_{ij} \frac{C_6^{\alpha\beta}}{R_{ij}^{\alpha\beta 6}} f(\mathbf{R}) \tag{2}$$

where the vdW strength coefficient, $C_6^{\alpha\beta}$, is calculated from atomic polarizabilities [11,5] using the Slater–Kirkwood approximation [12], modified in the present work by a scale factor, S_C, to facilitate a better fit to MP2 results for different functionals, and by a change of sign,

$$C_6^{\alpha\beta} = -S_C \times \frac{2C_6^\alpha C_6^\beta p_\alpha p_\beta}{p_\alpha^2 C_6^\alpha + p_\beta^2 C_6^\beta}. \tag{3}$$

The sum of vdW radii of two interacting atoms, $R_0^{\alpha\beta}$, is given by the "cubic-mean" rule [13], modified here by a second empirical and functional dependent scale factor S_R,

$$R_0^{\alpha\beta} = S_R \times \frac{(R_0^{\alpha\alpha})^3 + (R_0^{\beta\beta})^3}{(R_0^{\alpha\alpha})^2 + (R_0^{\beta\beta})^2}, \tag{4}$$

where $R_0^{\alpha\alpha} = 2 \times R_0^\alpha$ (R_0^α is the vdW radius of atom α).

The scale factors S_C and S_R are necessary to obtain a good fit of the vdW corrected results produced by different density functionals to the energy and geometry calculated at a high level, or to experimental results where they exist. Choices for the scale factors S_C and S_R are evaluated here for their effect on the binding energy, geometry, and the potential energy surface calculated for the methane dimer. These results are compared with experimental measurements, and with calculations on several other systems using very large basis sets at the MP2 and CCSD(T) levels.

2. Methods

In summary: (1) The interaction energy of two methane molecules is calculated as a function of the intermolecular distances for one orientation at the MP2/cc-pVQZ level. (2) The energy is calculated for the same configuration using DFT with and without empirical vdW corrections consisting of damped C6 potentials (Eqs. 1 and 2). (3) Parameters for the diatomic C6 coefficients and the damping function are calculated using Eqs. (3) and (4) using polarizabilities from Miller [11], except where we use strictly empirical parameters for the benzene type carbon introduced here. (4) Two scale factors, one for the C6 coefficients and one for the damping distance, are adjusted such that the DFT + vdW potential energy curve is similar to

the MP2/cc-pVQZ potential energy curve and the energy minimum comes close to the estimated MP2 and CCSD(T) complete basis set (CBS) limits. (5) Parameters using these scale factors are then used in calculations of DFT + vdW potential energy curves for dimers including ethane, ethylene, formaldehyde, ammonia, benzene, and water, and those results are compared with experimental, CCSD(T), and MP2 results obtained by others.

Results here are reported in units of angstroms and kcal/mol, while the input parameters are listed in the tables in A.U., Hartrees and Bohr. This apparent inconsistency was chosen, as a practical matter, to provide the units required for CPMD VDW input, while providing results in units that can be compared with those used in other papers on this subject.

The application of vdW corrections in the CPMD input includes all possible non-bonded interactions summed over one cell only.[1] While C6 coefficients for hydrogen are relatively small, Hydrogen can dominate these interactions because they are so numerous. We have not evaluated the effect of including partially charged hydrogen atoms as in the case of $-NH_3^+$.

The default behavior for the calculation of vdW energy in CPMD is to sum interactions between atoms in only one cell. The alternatives allow the inclusion of any number of cells along each axis. Except where explicitly noted here, where we have calculated inter-cell vdW interactions to test this feature of the code, and in calculations on cells containing one molecule, the default behavior was always used – summing the interaction energies between atoms in one cell only. This does not effect the non-vdW energies.

To provide a plot for the methane dimer potential energy surface (PES) at a reasonably high level, Dunning's correlation consistent, polarized valence, quadruple zeta basis, MP2/cc-pVQZ with counterpoise (CP) corrections, was used to scan the coordinate connecting the two carbon atoms using single point wave function optimization calculations. All MP2 calculations were performed using Gaussian 03 [16] with no PBC. The geometry for methane used in each of these calculations was obtained from a MP2/cc-pVQZ CP optimization of the methane dimer. The same geometry was also used in many single point scans of the PES using DFT/PBE and DFT/BLYP.

Dunning's MP2/aug-cc-pVXZ basis was also used to calculate the optimized methane dimer geometry [17]. It has been observed elsewhere that the uncorrected MP2/aug-cc-pVXZ series greatly overestimates binding energies in a comparison with the estimated CBS limit for the benzene dimer [18].

---

[1] For example, the input file for the benzene–water interaction included the following six lines: C6 1 2 − 1.30645 4.9024 3.0; C6 1 3 − 8.70145 5.0088 3.0; C6 2 2 − 2.29075 3.5376 3.0; C6 2 3 − 2.67495 3.9472 3.0; VDW-CELL; 0 0 0; where atom types 1, 2, and 3 are C, H, and O, respectively, determined from the order in which coordinates are listed in the ATOMS section.

Table 1
Comparison of DFT and MP2 calculations on the methane dimer, showing scale factors for the vdW input parameters, and optimized geometries and binding energies obtained from them

Method[a]	C–C	E_{attr}[b]	S_C[c]	S_R^{CC}[d]	S_R^{HH}[d]	S_R^{CH}[d,e]
PBE no vDW (1)	3.99	−0.17				
PBE + vDW(3)	3.72	−0.48	0.79	0.80	0.80	0.80
PBE + vDW(4)	3.80	−0.48	0.79	0.70	0.70	0.70
PBE + vDW(5)	3.71	−0.48	0.85	0.80	0.80	0.80
BLYP + vDW	3.67	−0.51	2.38	1.06	1.06	1.06
MP2/6–311 + G**	3.99					
MP2/cc-pVQZ[g]	3.72	−0.41				
MP2/aug-cc-pVQZ	3.65					
CBS limit[b]		−0.48				
CCSD(T) [14]	3.6	−0.50				
Best estimate[f]	3.67					

[a] Numbers in parenthesis indicate correspondence with curves in Fig. 1.

[b] Interaction energies are estimated as described in methods. E_{attr} for CH_4–CH_4 extrapolated to the basis set limit using CP corrected MP2/cc-pVQZ calculations at R = 3.8 Å (very near the minimum) is −0.48 kcal/mol [15].

[c] S_C, in Eq. (3), the scale factor applied to the theoretical diatomic vdW coefficients listed in column 1 of Table 2, is determined here by fitting the DFT PES for a particular density functional to the MP2 results. Optimal scale factors S_C and S_R were chosen by visual inspection of a large number of plots using different values for both.

[d] $S_R^{\alpha\beta}$, in Eq. (4), is the scale factor applied to the theoretical combined vdW radii listed in column 2 of Table 2 to fit the MP2 results. The "d" in Eq. (1), otherwise referred to as decay factor β, slightly shifts the damping function maximum to a smaller distance as it becomes much larger. "d" was set to 3.0 in all cases shown here. R_0 values used here are the standard vdW radii from Gavezzotti et al. [21,22,20] and, for mixed radii, calculated using the cubic mean rule [13], Eq. (4).

[e] The cc-pVQZ geometries were optimized using CP corrections. The aug-cc-pVQZ geometry was optimized without CP. For H-bonding interactions, the MP2 cc-pVQZ and aug-cc-pVQZ geometries have been shown to be within 0.01 Å of the complete basis set limit [26].

[f] The "best estimate" for the C–C distance is estimated from the optimized MP2/aug-cc-pVQZ geometry.

Table 1 represents the process for finding the scale factors S_C and S_R. Periodic boundary condition (PBC) DFT geometry optimizations of the methane dimer, using the vdW parameters listed in Table 1 with one exception, were performed to obtain the distances listed in the same table, using a 13.5 Å cubic cell. That exception was the use of Bondi's vdW radius for hydrogen, 1.2 Å [19]. Subsequent calculations using Gavezzotti's value, 1.17 Å [20–22], made no significant difference. Convergence criteria were set to 1.0E−6 for geometry and 1.0E−7 for orbitals (wave functions), and the optimizations were allowed to proceed for more than 100 geometry steps and until the maximum change in geometry was less than the precision used in Table 1. The conversion factor used to convert Hartrees to kcal/mol was 627.51 kcal/(H mol). PBC DFT optimizations using the same vdW parameters were also performed on ethane, using a 10.0 Å cubic cell with the same convergence criteria as described above, to test the effect of the vdW correction on bonded interactions.

It was not possible to calculate the interaction energy for a dimer at very large separation distances using PBC here. The cost of this calculation using plane waves increases dramatically with cell size, and a large number of calculations were required to test many combinations of scale factors for several density functionals. However, it is important to have a reasonably good estimate of this energy since the interaction curves are obtained by subtracting this value from the energies obtained at each separation distance, so that the curve is asymptotic with zero energy as the distance increases. This situation is complicated by the fact that many of the density functionals show significant positive interaction energy and repulsion at distances significantly greater than 6 Å [2]. This can distort the binding curves in PBC calculations, and this was the case in results using the BLYP functional. Another complication is added by the vdW interactions between atoms in adjacent cells. This problem is only partly eliminated by summing vdW energies over one cell since the CPMD vdW code still includes the interaction between two molecules in the same box as they approach each other across cell boundaries. A fuller analysis of the possible sources of error caused by using relatively small cells is included in the discussion section.

With these problems in mind, estimates of the binding energy were obtained by comparing two types of calculations: In the first, using the 13.5 Å cubic cell as an example, calculations were performed on a cell containing one centered molecule, summing vdW interactions over $1 \times 1 \times 1$ cells, providing the total energy for one molecule at a separation distance of 13.5 Å, but including no vdW interactions. The total energy from this calculation, multiplied by 2, was then subtracted from the total energies obtained from a series of calculations on the same cell containing two molecules.

In the second type, calculations were performed, for example, on a dimer in a $13.5 \times 27 \times 13.5$ Å orthorhombic cell at a separation of 13.5 Å where the long axis of the cell was parallel to the axis of separation. The total energy obtained from this calculation includes a small contribution from the vdW interaction, but was approximately equal to twice that obtained from the first type of calculation. The first type of calculation, costing less and being more accurate, was generally preferred.

As the separation between two molecules in a cell increases, the separation between these molecules across cell boundaries decreases, and the error introduced by this trade-off here reaches a maximum at a separation equal to half the cell dimension along the separation axis. This particular interaction occurs even when other vdW interactions across cell boundaries are avoided by summing vdW energies over only one cell. However, using a 13.5 Å cubic cell, this error is a small fraction of the binding energy minimum using the PBE functional. (This could not be achieved with BLYP.) For example, the methane dimer in the 13.5 Å cubic cell has an interaction energy of about −0.025 kcal/mol at a separation of 6.75 Å. This is roughly two times the actual interaction energy, so the error in the binding plot here would be about 0.013 kcal/mol at 6.75 Å, 2.6% of the minimum binding energy.

To test the effect of the vdW correction across cell boundaries where vdW energies are summed in only one cell, a series of calculations were performed with two methane molecules per cubic cell, where molecules were placed binding to each other in the D3d configuration across cell boundaries. Results were the same as those shown in Fig. 1.

The optimization of scale factors, and the DFT binding curves for dimers of methane, ethane, ethylene, formaldehyde, ammonia, the benzene sandwich dimers, and for the benzene–water interaction, were obtained using the 13.5 Å cubic cell. DFT binding curves shown here for the benzene T dimer used an orthorhombic cell $11 \times 20 \times 11$ Å where zero binding energy was estimated from the energy at a separation of 10 Å. A discussion of the possible errors introduced by the 11 Å cell dimension is included below.

All DFT calculations were performed using CPMD [23]. Troullier-Martins [24] norm conserving pseudopotentials were used throughout.[2] The integration scheme for non-local parts of the pseudopotentials was Kleinman-Bylander [25] in all cases. Several different norm conserving carbon pseudopotentials are available for the BLYP density functional. Two tested here gave nearly identical results. Most results shown here were produced using an energy cut-off of 120 Ry. However, subsequent repeated calculations using a cut-off of 80 Ry gave results that were virtually identical to those using 120 Ry.

3. Results and discussion

3.1. Methane and ethane

Figs. 1 and 2 show geometries and the calculated PES for methane and ethane dimer binding coordinates. Table 1 shows a representation of the process for finding the vdW parameter scale factors, S_C and S_R in Eqs. (3) and
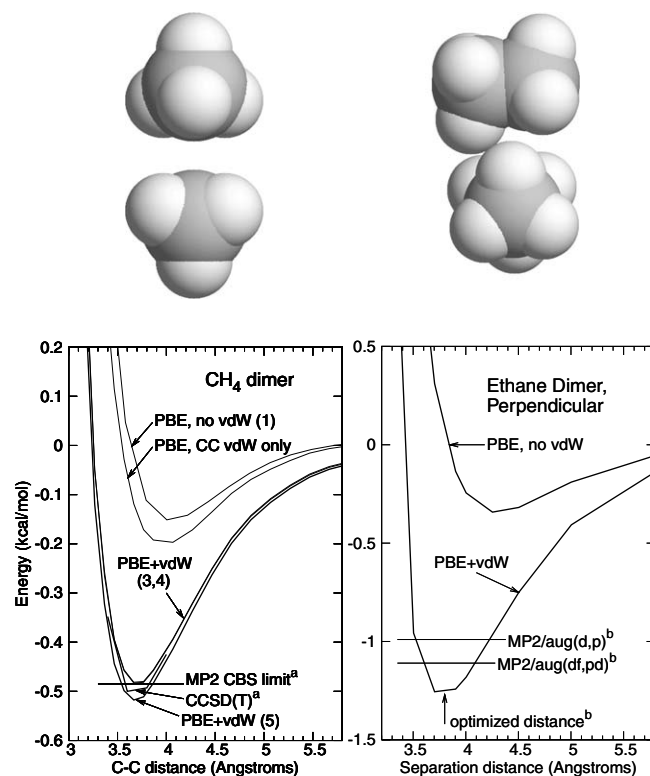

Fig. 1. *Top:* Geometry for the methane D_{3d} and ethane C_2 dimers. *Bottom left:* Potential energy curves for the CH_4 dimer, with and without vdW corrections for the PBE functional, compared with CCSD(T)/aug(df,pd)-6–311G** results and the estimated MP2 complete basis set (CBS) limit from [a]Tsuzuki and Luthi [14]. The numbers in parenthesis indicate correspondence with sets of parameters listed in Table 1. Curve (3), where $S_C = 0.79$, represents the best fit to the binding energy at the CBS limit (−0.48 kcal/mol), whereas curve (5), where $S_C = 0.85$, is closer to the CCSD(T) results. The damping function in Eq. (1) appears to combine in a fortuitous way with the PBE functional to produce binding curves that reproduce the MP2 results. A plot of some of these curves extended to 13 Å can be seen in Fig. 2. *Bottom right:* Similar results using $S_C = 0.85$ are shown for the perpendicular ethane dimer, compared with MP2/aug(d,p)-6–311G** and MP2/aug(df,pd)-6–311G** results from [b]Tsuzuki et al. [15].

(4), and resulting bonding distances and energies. Table 2 shows lists of values for $C_6^{\alpha\beta}$ calculated from Tables 1 and 2 in Elstner et al. [5], and for $R_0^{\alpha\beta}$ calculated using vdW radii from Gavezzotti et al., [21,22,20]. vdW radii from Bondi [19] gave nearly the same results. The parameters recommended here are those that produce the curve labeled PBE + vdW(5), where the binding energy is near −0.52 kcal/mol and the optimized C–C distance is 3.71 Å.

Molecules in the simulation cell also interact with molecules in adjacent cells. Errors from these unintended interactions can be important where the non-vdW interaction energies are relatively large, and where the dimensions of the cell are too small. There are two sources for these errors: (1) from vdW interactions, and (2) from the density functionals themselves. The most significant unwanted contribution from vdW interactions across cell boundaries has been avoided here by summing vdW energies between atoms in only one cell.
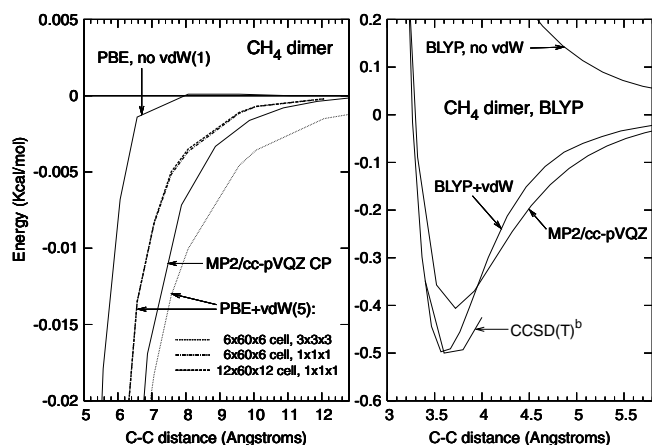
Fig. 2. *Left:* Potential energy curves for the CH_4 dimer between 5 and 13 Å using a 13.5 Å cubic cell (PBE, novdW(1)), and two orthorhombic cells: $6 \times 60 \times 6$ and $12 \times 60 \times 12$ Å, that include a summation of the vdW energy over $1 \times 1 \times 1$ cells, or over $3 \times 3 \times 3$ cells. The curve for the uncorrected PBE calculation rises slightly above zero around 8 Å before it returns with more distance to zero. This behavior in PBE is much less pronounced than it is in many other density functionals [2], making it a good candidate for vdW correction. Where vdW energies are summed over only one cell, the PBE curves are nearly identical and show regular asymptotic behavior in cells with very different dimensions. The summation over $3 \times 3 \times 3$ cells shows the effect of including inter-cell vdW corrections, not desired here. The uncorrected BLYP curve (not shown) is off scale above zero here, and the vdW corrected curves in different cells show differences on the order of 0.01–0.02 kcal/mol, systematic errors due to non-vdW interactions with molecules in adjacent boxes. *Right:* B3LYP Potential energy curves for the CH_4 dimer in a 13.5 Å cubic box, with and without vdW corrections, compared with MP2 calculations performed here and with CCSD(T)/aug(df,pd)-6–311G** results from [b]Tsuzuki and Luthi [14]. BLYP, which has given good results when corrected using a different damping function [7], does not behave well with the damping function and periodic boundary condition (PBC) cell sizes used here. The MP2 and CCSD(T) results were obtained using non-PBC calculations.

Calculations were performed to illustrate how vdW summation over one cell avoids this systematic error. The vdW corrected curves shown in Fig. 2 were obtained in three calculations: (1) using a $6 \times 60 \times 6$ Å cell with vdW summation over $3 \times 3 \times 3$ cells, (2) using a $6 \times 60 \times 6$ Å cell with vdW summation over $1 \times 1 \times 1$ cells, and (3) using a $12 \times 60 \times 12$ Å cell with vdW summation over $1 \times 1 \times 1$ cells. The two curves representing sums over $1 \times 1 \times 1$ cells are nearly identical, differing only by the interactions represented by the "PBE, no vdW" curve. The curve representing a sum over $3 \times 3 \times 3$ cells shows behavior that in this case is undesirable. Summation over a minimum of $3 \times 3 \times 3$ cells would be required in normal PBC calculations on molecular crystals.

The same calculations were performed using the BLYP density functional. The curves produced by the two calculations: (1) using a $6 \times 60 \times 6$ Å cell with vdW summation over $1 \times 1 \times 1$ cells, and (2) using a $12 \times 60 \times 12$ Å cell with vdW summation over $1 \times 1 \times 1$ cells, showed very large differences, on the order of 0.01–0.02 kcal/mol. The distortion observed in the BLYP + vdW curve shown in Fig. 2 right near 4.5 Å is probably caused by this undesired interaction

represented by the positive and non-asymptotic part of the "BLYP, no avdW" curve near 7.5 Å (off scale and not shown).

The curve labeled "PBE, CC vdW only" in Fig. 1 was obtained by including only the CC interaction in the vdW correction. Clearly, the CH and HH interactions are at least as important as the CC. Although the diatomic coefficients, $C_6^{\alpha\beta}$, for CH and HH interactions are a magnitude smaller than that for CC, there are six HH and six CH interactions in CH_4–CH_4, and the distances in these cases are smaller than that between the two carbon atoms.

It is important that the VDW corrections should have no effect on normal bonded interactions. The Elstner et al. choice for damping function exponents yields a function that is essentially zero below about 2.5 Å, as can be see in their Fig. 1 [5]. It should be expected that molecules optimized with the same convergence criteria, with and without VDW corrections, should have essentially the same normal

Table 2
Diatomic $C_6^{\alpha\beta}$ coefficients (Hartree · Bohr[6]) and combined vdW radii, $R_0^{\alpha\beta}$ (Bohr), for the PBE functional calculated with scale factors applied[a]

Atom types[b]	$C_6^{\alpha\beta}$	$R_0^{\alpha\beta}$	Atom types[b]	$C_6^{\alpha\beta}$	$R_0^{\alpha\beta}$
H–H	−2.290	3.538	N_{TR2}–H	−1.692	4.158
C_{TE}–H	−1.644	4.625	N_{TR2}–N_{TR2}	−18.721	4.535
C_{TE}–C_{TE}	−18.394	5.140	N_{TR2}–N_{PI2}	−19.440	4.535
C_{TR}–C_{TR}	−26.403	5.140	N_{TR2}–O_{TR4}	−7.925	4.395
C_{AR}–C_{AR}	−49.790	5.473	N_{TR2}–O_{TE}	−9.954	4.395
C_{AR}–O_{TE}	−8.702	5.009	N_{PI2}–O_{TR4}	−3.494	4.395
C_{TE}–O_{TR4}	−7.731	4.773	N_{PI2}–O_{TE}	−3.606	4.395
C_{TE}–O_{TE}	−9.728	4.773	N_{PI2}–H	−1.371	4.158
C_{TR}–H	−1.302	4.625	N_{PI2}–N_{PI2}	−2.882	4.535
C_{AR}–H	−1.306	4.902	O_{TR4}–O_{TR4}	−8.123	4.233
C_{TE}–C_{TR}	−20.202	5.140	O_{TR4}–O_{TE}	−8.674	4.233
C_{TE}–N_{TR2}	−18.553	4.875	O_{TR4}–H	−2.756	3.947
C_{TE}–N_{PI2}	−19.305	4.875	O_{TE}–O_{TE}	−9.631	4.233
C_{TR}–N_{TR2}	−20.208	4.875	O_{TE}–H	−2.675	3.947
C_{TR}–N_{PI2}	−21.886	4.875	S_{TE}–S_{TE}	−127.206	5.594
C_{TR}–O_{TR4}	−6.484	4.773	S_{TE}–H	−0.591	5.006
C_{TR}–O_{TE}	−8.395	4.773	S_{TE}–C_{TE}	−12.779	5.386
N_{TE}–H	−1.805	4.158	S_{TE}–C_{TR}	−22.835	5.386
N_{TE}–N_{TE}	−19.489	4.535	S_{TE}–C_{AR}	−41.572	5.534

[a] $C_6^{\alpha\beta}$ is calculated as described by Elstner et al. [5] using Eq. (3) above and polarizabilities from Miller [11], except in the case of parameters for C_{AR} which were obtained by fitting the binding curves for benzene dimers. $R_0^{\alpha\beta}$ is calculated from the vdW radii provided by Gavezzotti and coworkers [21,22,20] (H, 1.17; O, 1.40; N, 1.50; C, 1.70 Å) using Eq. (4). Unscaled values use $S_C = S_R = 1.0$. Scale factors use here: for PBE, $S_C = 0.85$ and $S_R = 0.80$. Not used in this table, scale factors for BLYP are $S_C = 2.37$ and $S_R = 1.06$.
[b] Atom types are from Miller's Table 1 [11] except where noted: C_{TE}, tetrahedral carbon; C_{TR}, trivalent carbon where one bond is doubled or where two bonds share a conjugated double bond; C_{AR}, not from Miller, aromatic carbon parameters constructed in this work specifically to fit the potential energy curves for the benzene dimer; N_{TE}, tetrahedral nitrogen with three s bonds and one free electron pair, as in ammonia; N_{TR2}, trivalent nitrogen with two bonds sharing a conjugated double bond and one free pair of electrons; N_{PI2}, nitrogen with three bonds where two share a conjugated double bond, or where one bond is double, as in an amide group; O_{TE}, oxygen with two bonds and two free electron pairs, as in alcohols; O_{TR4}, oxygen with one double bond and two free electron pairs, as in a carbonyl group. For other atom types see Miller.

bond distances and energies, and this is the case here. For example, CC bond distances for isolated ethylene, optimized using CPMD with and without VDW correction, were 1.528448 and 1.528436 Å, respectively, different by 1×10^{-5} Å, and total energies were -14.958093 -14.957879 Hartrees, respectively, different by 0.13 kcal/mol, indicating that vdW corrections using this damping function in CPMD are sufficiently limited to non-bonded interactions.

3.2. Ethylene, formaldehyde, and ammonia

Fig. 3 shows binding energy curves for dimers of ethylene, formaldehyde, and ammonia. For ammonia the repulsion energy is about 0.3 kcal/mol lower than the extrapolated MP2 CBS limit. Otherwise, the vdW corrected PBE results are within 0.1 kcal/mol of the CCSD(T) results or the MP2 CBS limit. The PBE + vdW separation distance for the ethylene dimer appears to be about 0.15 Å shorter than that predicted by the CCSD(T) results, suggesting that the vdW radius or S_R could be larger for the C_{TR} atom type than it is for C_{TE}. As shown below, it was necessary to assume a larger vdW radius for the C_{AR} atom type in order to fit the experimental and MP2 separation distances for the benzene dimer.

3.3. The benzene dimer

Fig. 4 shows binding energy curves for the benzene dimer in three geometries. Sinnokrot et al. [18] observed that MP2 results, using a variety of very large basis sets augmented with diffuse functions and polarized basis sets, significantly overestimate the binding energy for all three configurations with respect to the estimated CCSD(T) CBS limit. In this respect, the vdW corrected DFT/PBE results are superior to MP2 calculations in every case here. Also, the vdW corrected PBE results for the separation distance matches those of the experimental [28] and MP2 results within 0.05 Å using the C_{AR} atom type.

The desirable asymptotic behavior shown in Fig. 2 left, with negligible non-vdW interaction energy above 8 Å for the PBE functional, combined with the absense of inter-cell vdW interactions in this case, insures that the relatively small cell sizes used here introduce only small errors. The worst case scenario is provided by the benzene parallel sandwich dimer at a separation of 3.8 Å in the $11 \times 20 \times 11$ cell (Fig. 4). The distance between translation symmetry related interaction neighbors is then $\sqrt{3.8 \times 3.8 + 11 \times 11} = 11.6$ Å, where the total interaction energy is negligible. Even at 7.3 Å the total inter-cell interaction for the parallel displaced sandwich is about
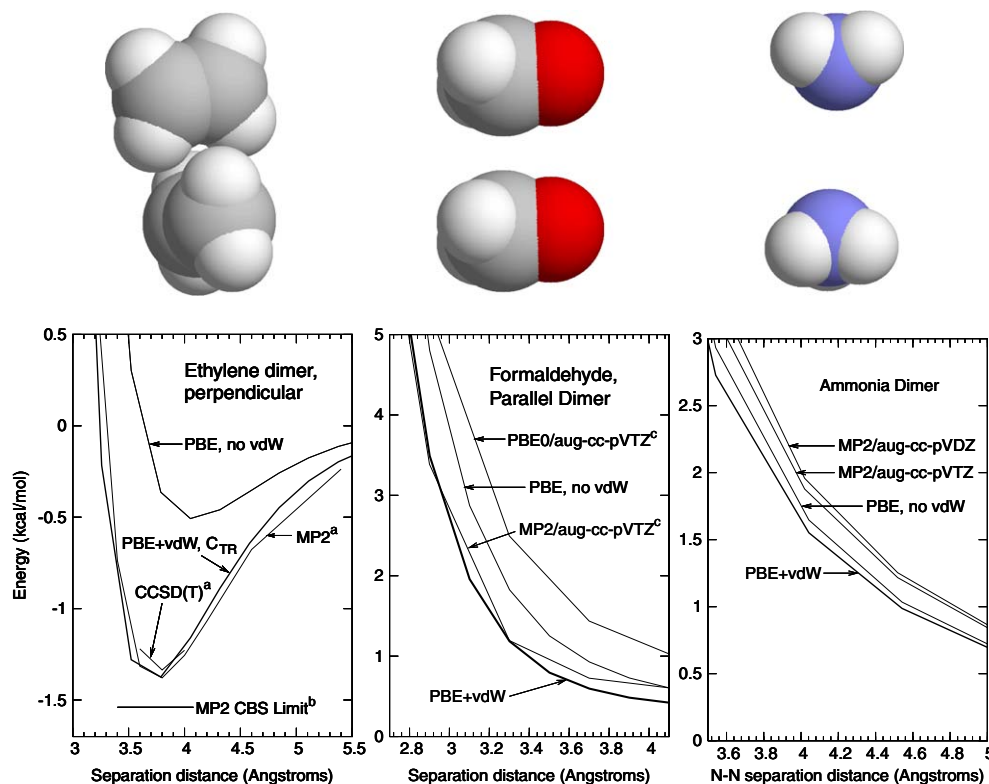

Fig. 3. *Top:* Geometries for the ethylene, formaldehyde, and ammonia dimmers. *Bottom:* Potential energy curves for the ethylene, formaldehyde, and ammonia dimers, with and without vdW corrections for the PBE functional. For ethylene, comparisons are made with MP2/aug(df,pd)-6–311G** and CCSD(T)/aug(df,pd)-6–311G** results from [a]Tsuzuki and Luthi [14], and with the estimated MP2 CBS from [b]Tsuzuki et al. [15]. For formaldehyde, comparisons are made with PBE0/aug-cc-pVTZ and MP2/aug-cc-pVTZ results from [c]Improta and Barone [1]. For ammonia, where the N–H bonds on each molecule point away from each other, comparisons are made with MP2/aug-cc-pVXZ series calculations performed here.
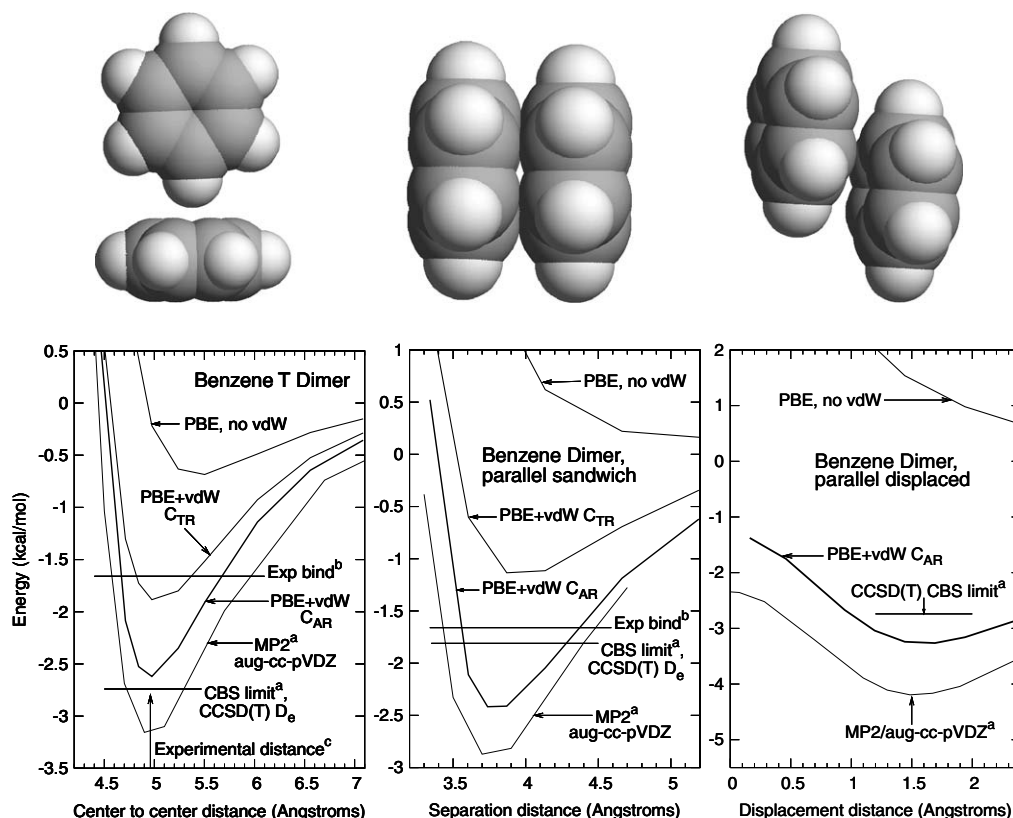
Fig. 4. *Top:* Geometries for the benzene T dimer, sandwich, and slipped sandwich. *Bottom:* PBE Potential energy curves for the benzene T, sandwich, and parallel displaced dimers, with vdW corrections, compared with counterpoise corrected MP2/aug-cc-pVDZ results and the estimated CCSD(T) CBS limit from [a]Sinnokrot et al. [18]. The center to center distance, R_C, is measured from the centroid of each molecule. Not shown here, the MP2/aug-cc-pVTZ results show an even greater binding energy, and MP2 calculations in general, including those with other large basis sets, significantly overestimate the binding energy of these dimers with respect to the estimated CCSD(T) CBS limit and experimental results. For the parallel displaced dimer, the constant separation of 3.5 Å is measured as the distance between the planes of each molecule along a line normal to those planes, R_N, and the displacement distance, R_D, is measured as $R_D = \sqrt{R_C^2 - R_N^2}$. [b]Experimental measurements of the benzene dimer binding energy, where geometry was not modeled, have yielded a value of -1.66 ± 0.16 kcal/mol[27]. [c]Experimental measurements of the gas phase benzene T dimer separation found a distance of 4.96 Å [28].

+0.05 kcal/mol, representing a 5% error in the "PBE + vdW C_{TR}" curve.

3.4. Benzene–water

In the context of their study of the benzene–water inter-action, and without further analysis with respect to benzene dimer geometry, Courty et al. [27] report an experimental measurement of the benzene dimer binding energy at -1.66 ± 0.16 kcal/mol. This is significantly lower than that obtained for the CCSD(T) CBS limit near -2.7 kcal/mol for the T geometry, but it is within 0.2 kcal/mol of that limit for the sandwich and parallel displaced dimers. With respect to predicting the experimental binding energy, the vdW corrected PBE results using the C_{TR} atom type are comparable to those at the CCSD(T) CBS limit.

Evaluating the effects of dispersion correction on six different DFT functionals using several different combinations of damping and combination functions, Zimmerli et al. [9] report that dispersion corrected PBE and B3LYP functionals generally show much improved results.

Fig. 5 shows binding energy curves for the benzene–water interaction in three geometries. Comparisons are made with MP2 and the best vdW corrected results using unscaled parameters from Zimmerli et al. [9], the experimentally measured distance for the water down geometry from Suzuki et al. [29], and experimental measurements of the benzene–water binding energy from Cheng et al. [30], and Courty et al. [27]. For the water-up geometry, the vdW corrected DFT results are at best 0.6 kcal/mol lower than those from MP2, and the two PBE results are essentially the same. For the water-parallel geometry, the scaled vdW correction parameters show a significant improvement over the unscaled parameters, being about 0.3 kcal/mol lower than the MP2 results. For the water-down geometry, the scaled parameters yield a separation distance that is within 0.03 Å of the experimentally measured distance and that is about 0.2 kcal/mol from experimentally measured binding energy. The unscaled parameters yield a distance that is about 0.1 Å too high, but correctly predicts the experimental binding energy. Overall, the scaled vdW parameters perform marginally better than do the
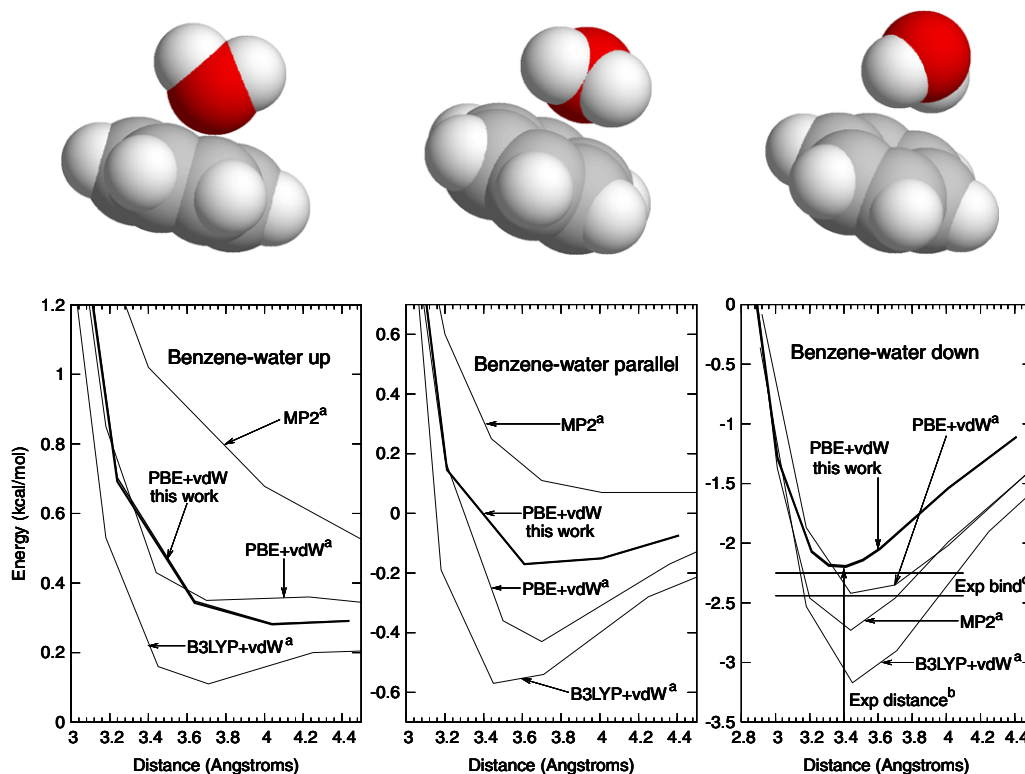
Fig. 5. *Top:* Geometries for benzene–water up, parallel, and down configurations. *Bottom left:* vdW corrected PBE potential energy curves for benzene–water in the up (water hydrogens turned away from benzene), parallel, and down (water hydrogens toward benzene) geometries. vdW corrections for both C_{AR} and (for the up and down geometries) C_{TR} atom types yield virtually identical results here where the curves are indistinguishable. These are compared with three results from [a]Zimmerli et al. [9]: (1) vdW corrected PBE results using damping and combination Eqs. (1) and (3) with no scaling, (2) vdW corrected B3LYP DFT results using their number 9 and 11 damping and combination equations described by Wu and Yang [6], and (3) counterpoise corrected MP2/6–311G(2d,2p) results. [b]Experimental microwave measurements of the gas phase benzene–water distance [29], measured from the center of mass of both molecules, is 3.32 Å using a model where θ, the angle between the C_6 axis of benzene and the C_2 axis of water, the same geometry described here as "water down", is 0°. The benzene centroid to water oxygen atom distance is 0.08 Å longer than the center of mass distance, and it is this distance to the oxygen atom that is indicated in the figure. [c]Experimental measurements of the benzene–water binding energy found 2.25 ± 0.28 kcal/mol [30], and 2.44 ± 0.09 kcal/mol [27].

unscaled values, and with respect to the experimental results for the stable geometry the vdW corrected PBE results are superior to MP2 using the 6–311G(2d,2p) basis.

Table 3
Comparison of dispersion coefficients, $C_6^{\alpha\beta}$, in Hartree · Bohr[6], developed by different groups

Source[a]	H–H	C_{TR}–C_{TR}	C_{TR}–H	O_{TE}–O_{TE}	C_{TR}–O_{TE}
This work	2.29	26.4	1.30	9.63	8.40
Zimmerli et al. [9]	2.83	32.6	1.61	11.86	10.34
Wu and Yang [6]	2.83	27.4	1.61	11.61	10.00
Elstner et al. [5]	2.69	31.1	1.53	11.33	11.44

[a] The $C_6^{\alpha\beta}$ coefficients here are calculated using polarizabilities from Miller [11] and on the $C_6^{\alpha\alpha}$ coefficients given in the various sources. As shown in Table 2, coefficients for C_{AR}–H and C_{AR}–O_{TE} interactions are 1.306 and 8.70, respectively, still significantly lower than those used by other groups. Although the C_{AR}–C_{AR} coefficient is quite high at 49.8, the combination rule (Eq. 3) applied to C_{AR} combined with other atom types yields a low figure that is consistent with the MP2 and CCSD(T) results. Not shown here, values for $R_0^{\alpha\beta}$ are also significantly smaller than those used by other groups.

4. Conclusions

Two scale factors are used here, one for C_6 coefficients and one for vdW radii, that provide flexibility in the tailoring and application of empirical vdW corrections to specific atomic interactions, damping functions, and density functionals in DFT codes, specifically here for CPMD. The resulting parameters are significantly smaller than those used by other groups, as is shown in Table 3. Where experimental and CCSD(T) results can be used as a standard, these parameters produce results for a relatively diverse set of model interactions that are generally superior to those obtained at the MP2 level using large basis sets.

References

[1] R. Improta, V. Barone, J. Comput. Chem. 25 (2004) 1333.
[2] E. Johnson, R. Wolkow, G. DiLabio, Chem. Phys. Lett. 394 (2004) 334.
[3] J. Dobson, J. Wang, Phys. Rev. Lett. 82 (10) (1999) 2123.
[4] X. Xu, W.A. Goddard III, Proc. Natl. Acad. Sci. 101 (9) (2004) 2673.
[5] M. Elstner, P. Hobza, T. Frauenheim, S. Suhai, E. Kaxiras, J. Chem. Phys. 114 (12) (2001) 5149.

[6] Q. Wu, W. Yang, J. Chem. Phys. 116 (2) (2002) 515.
[7] S. Grimme, J. Comp. Chem. 25 (12) (2004) 1463.
[8] M.A. Neumann, M.-A. Perrin, J. Phys. Chem. B. 109 (2005) 15531.
[9] U. Zimmerli, M. Parrinello, P. Koumoutsakos, J. Chem. Phys. 120 (6) (2004) 2693.
[10] W.T.M. Mooij, F.B. van Duijneveldt, J.G.C.M. van Duijneveld-van de Rijdt, B.P. van Eijck, J. Phys. Chem. A 103 (1999) 9872.
[11] K.J. Miller, J. Am. Chem. Soc. 112 (1990) 8533.
[12] J. Slater, J.G. Kirkwood, Phys. Rev. 37 (1931) 682.
[13] T. Halgren, J. Am. Chem. Soc. 114 (1972) 7821.
[14] S. Tsuzuki, H.P. Lüthi, J. Chem. Phys. 114 (9) (2001) 3949.
[15] S. Tsuzuki, T. Uchimaru, M. Mikami, K. Tanabe, J. Phys. Chem. A 102 (12) (1998) 2091.
[16] M.J. Frisch, G.W. Trucks, H.B. Schlegel, G.E. Scuseria, M.A. Robb, J.R. Cheeseman, J.A. Montgomery Jr., T. Vreven, K.N. Kudin, J.C. Burant, J.M. Millam, S.S. Iyengar, J. Tomasi, V. Barone, B. Mennucci, M. Cossi, G. Scalmani, N. Rega, G.A. Petersson, H. Nakatsuji, M. Hada, M. Ehara, K. Toyota, R. Fukuda, J. Hasegawa, M. Ishida, T. Nakajima, Y. Honda, O. Kitao, H. Nakai, M. Klene, X. Li, J.E. Knox, H.P. Hratchian, J.B. Cross, C. Adamo, J. Jaramillo, R. Gomperts, R.E. Stratmann, O. Yazyev, A.J. Austin, R. Cammi, C. Pomelli, J.W. Ochterski, P.Y. Ayala, K. Morokuma, G.A. Voth, P. Salvador, J.J. Dannenberg, V.G. Zakrzewski, S. Dapprich, A.D. Daniels, M.C. Strain, O. Farkas, D.K. Malick, A.D. Rabuck, K. Raghavachari, J.B. Foresman, J.V. Ortiz, Q. Cui, A.G. Baboul, S. Clifford, J. Cioslowski, B.B. Stefanov, G. Liu, A. Liashenko, P. Piskorz, I. Komaromi, R.L. Martin, D.J. Fox, T. Keith, M.A. Al-

Laham, C.Y. Peng, A. Nanayakkara, M. Challacombe, P.M.W. Gill, B. Johnson, W. Chen, M.W. Wong, C. Gonzalez, J.A. Pople, Gaussian 03, Revision C.02, Gaussian, Inc., Wallingford, CT, 2004.
[17] T. van Mourik, A.K. Wilson, K.A. Peterson, D.E. Woon, T.H. Dunning, Adv. Quant. Chem. 31 (1999) 105.
[18] M.O. Sinnokrot, E.F. Valeev, C.D. Sherrill, J. Am. Chem. Soc. 124 (2002) 10887.
[19] A. Bondi, J. Phys. Chem. 68 (1964) 441.
[20] J.D. Dunitz, A. Gavezzotti, Acc. Chem. Res. 32 (8) (1999) 677.
[21] A. Gavezzotti, J. Am. Chem. Soc. 105 (16) (1983) 5220.
[22] G. Filippini, A. Gavezzotti, Acta Crystallogr. Sect. B: Struct. Sci. 49 (5) (1993) 868.
[23] CPMD Version 3.9.1, Copyright IBM Corp 1990–2004, Copyright MPI für Festkörperforschung Stuttgart 1997–2001. Available from: http://www.cpmd.org/.
[24] N. Troullier, J.L. Martins, Phys. Rev. B 43 (1991) 1993.
[25] L. Kleinman, D.M. Bylander, Phys. Rev. Lett. 48 (1982) 1425.
[26] B. Paizs, P. Salvador, A.G. Császár, M. Duran, S. Suhai, J. Comput. Chem. 22 (2) (2001) 196.
[27] A. Courty, M. Mons, I. Dimicoli, F. Piuzzi, M.-P. Gaigeot, V. Brenner, P.d. Pujo, P. Millié, J. Phys. Chem. A 102 (1998) 6590.
[28] E. Arunan, H.S. Gutowsky, J. Chem. Phys. 98 (1993) 4294.
[29] S. Suzuki, P.G. Green, R.E. Bumgarner, S. Dasgupta, W.A. Goddard III, G.A. Blake, Science 257 (1992) 942.
[30] B.M. Cheng, J.R. Grover, E.A. Walters, Chem. Phys. Lett. 232 (1995) 364.